Transactions of the Royal Society of Edinburgh: Earth Sciences, **97**, 325–336, 2008 (for 2006)

Impact of melt segregation on tonalite–trondhjemite–granodiorite (TTG) petrogenesis

Tracy Rushmer and Matt Jackson

"In searching for the origin of granites, it is tempting to view them as purely chemical systems"
(Pitcher 1979, p. 90)

ABSTRACT: Although sophisticated geochemical studies tell us that tonolite–trondhjemite–granodiorite (TTG) plutonic complexes must be formed by partial melting of metabasaltic source material, they cannot tell us the tectonic regime in which this crust was formed, nor how large volumes of TTG magma can be generated. This study suggests that a solution to TTG arc crust formation requires a strongly interdisciplinary approach, to resolve the tectonic setting (slab melt verses mafic lowermost crust sources), the time and length scales for melting and extraction, and the role of melt segregation mechanisms in the formation of both Archean TTGs and more recent adakite-like magmas. The aim of this paper is to present an experimental approach which, when coupled with numerical models, allows some of these issues to be addressed. The experiments are designed to reproduce the local changes in bulk composition that are predicted to occur in response to buoyancy-driven melt segregation along grain edges and associated compaction of the solid residue. The preliminary study presented here documents the changes we observe in the melt composition and melt and solid phase modes between earlier direct partial melting and the new segregation equilibration experiments on metabasalt bulk compositions. The results suggest that if dynamic melt segregation and equilibrium processes are active, they may modify the normally robust geochemical indicators, such as Mg-numbers, which are typically used to develop models of TTG petrogenesis.

KEY WORDS: Experimental petrology, metabasalt, numerical modelling, partial melting

Tonalite–trondhjemite–granodiorite (TTG) and associated rock types comprise a significant portion of the continental crust (Davidson & Arculus 2006; McLennan *et al.* 2006), and provide a window into the origin of Earth's earliest crust, the role of the mantle wedge, and the thermal regimes present in both early Earth and post-Archean subduction zones (Peacock *et al.* 1994; Martin 1999; Martin *et al.* 2005; Rollinson 2006). However, while we know that granites and similar arc rocks are commonly produced during partial melting in the lowermost crust, and that migration and emplacement at higher levels is how the crust normally differentiates and evolves, TTG magmatism is an enigma because the tectonic setting in which the basaltic source material undergoes partial melting is still unresolved (Drummond & Defant 1990; Atherton & Petford 1993; Petford & Atherton 1996). Partial melting of the down-going slab is a preferred model for Archean TTGs, because higher heat flow in the early Earth enhances the potential ranges for slab melting scenarios (e.g. Martin 1999; Martin *et al.* 2005), but thermal and physical models of post-Archean subduction zones suggest that extensive magma generation from the downgoing slab may be difficult or impossible except in very young oceanic crust, or possibly in slabs with a low subduction angle (e.g. Peacock *et al.* 1994; Kincaid & Sacks 1997; Gutscher *et al.* 2000). However, thermal modelling using temperature-dependent mantle viscosities suggests that older crust (50–60 My) might allow melting, particularly if fluid is present (Kelemen *et al.* 2003). Most difficult, however, is that it has not been possible to use geochemically-driven models to determine the tectonic environment for the origin of TTG magmas, whether they are generated from the downgoing plate during subduction or during underplating events. Slab sources and mafic lowermost crust sources are both viable in terms of PTx conditions to produce the signature TTG major and minor element ratios (e.g. Sr/Y >40 ppm, depleted HREE, $(La/Yb)_N$ >10 ppm), of which the presence of garnet and amount of plagioclase is key (Drummond & Defant 1990; Rapp & Watson 1995).

A significant problem in understanding the origin of TTG magma bodies is that we do not know the physical mechanism by which the melt segregates from its source rock, and how this might affect the chemistry of the segregated melt. During melting, the solid fraction maintains an interconnected matrix until the melt volume fraction exceeds a threshold at which the matrix disaggregates and a mobile magma forms. The present authors use the 'Critical Melt Fraction' or CMF term (equivalent to the solid-to-liquid transition (SLT) of Rosenberg & Handy (2005)) to describe the melt fraction at which the dominant rheology (at low strain rates) changes from a matrix containing interstitial melt, to a dilute suspension (magma). The CMF lies most likely in the range of 35–50% melt (van der Molen & Paterson 1979; Petford 2003; Rosenberg & Handy 2005), which is generally higher than TTG partial melt fractions in basaltic (amphibolitic to eclogitic transition) source rocks (c. 5–30%; see Beard & Lofgren 1991; Rapp *et al.* 1991, 1999; Rushmer 1991; Wolf & Wyllie 1994; Rapp & Watson 1995). To form a mobile, relatively crystal-free magma which can migrate away from the source region, the melt must therefore flow relative to the solid matrix and accumulate until

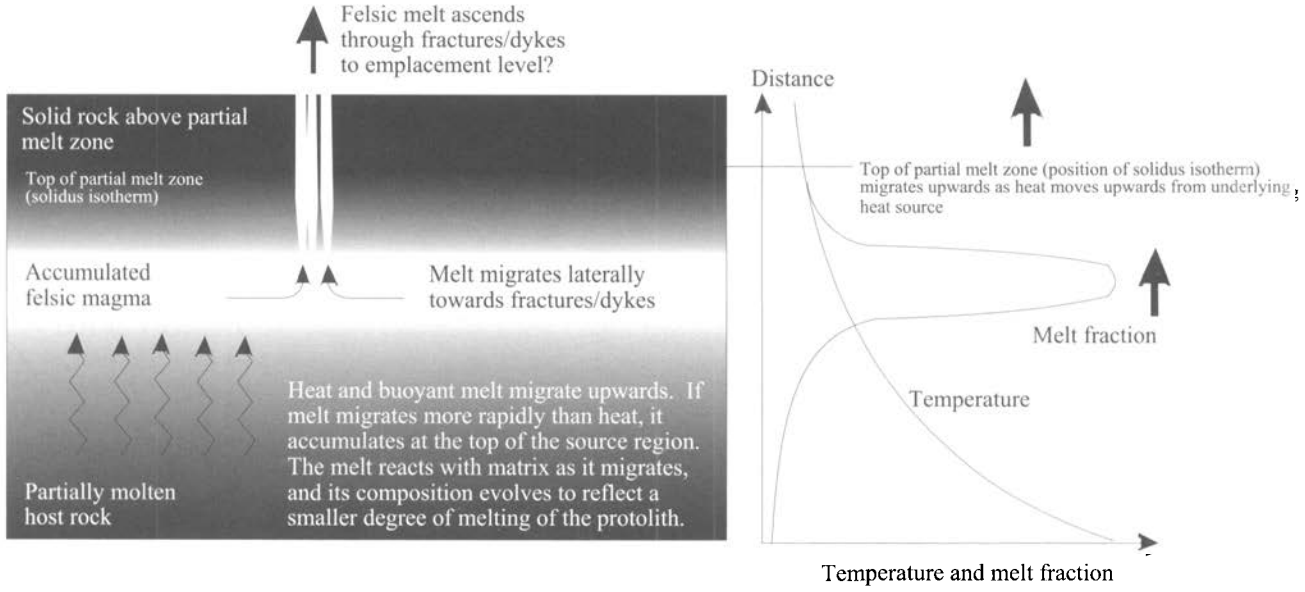

Figure 1 Felsic partial melt may segregate from a mafic host during buoyancy driven compaction of the matrix (Jackson *et al.* 2003, 2005). Previous studies have suggested that this segregation mechanism is too slow (e.g. McKenzie 1984; Richter & McKenzie 1984; Wickham 1987) to yield large volumes of felsic melt, but neglected the chemical interaction between it and its matrix.

it exceeds the CMF. This process is termed melt segregation (e.g. Wickham 1987; Brown 1994; Sawyer 1994, 1996). Melt must initially flow along grain boundaries where it is formed during melting, and as it does so is likely to chemically interact with the solid matrix. The problem is that the physical mechanism by which large-scale segregation occurs, and the resulting influence on melt chemistry during segregation, is poorly understood.

Melt segregation requires that the partially molten rock matrix is permeable, that there is a fluid potential gradient to drive melt flow relative to the matrix, and that there is space available to accommodate the melt (Jackson *et al.* 2003, 2005). The available evidence suggests that partially molten basaltic source rocks are permeable, with melt connected along grain boundaries, even at low (<0·04) porosities (e.g. von Bargen & Waff 1986; Cheadle 1989; Wolf & Wyllie 1991, 1994; Vincenzi *et al.* 1998; Wark & Watson 1998; Lupulescu & Watson 1999; this is the 'melt connectivity transition' (MCT) of Rosenberg & Handy 2005). If the source rock is layered, and the layers have different rheological properties, then tectonically driven deformation can provide both a potential gradient and accommodation space. Because the layers respond differently to deformation, potential gradients form between them and space is created at dilatant sites such as boudins and fractures (e.g. Brown 1994; Sawyer 1994, 1996; Brown *et al.* 1995, Brown & Rushmer 1997). Melt migration can also be driven by buoyancy, either along grain boundaries or through a network of fractures (e.g. McKenzie 1984; Wickham 1987; Petford 1995; Petford & Koenders 1998; Rushmer 2001). If flow occurs along grain boundaries, then melt enhanced diffusional creep processes provide a mechanism for changing the morphology of the grains (Pharr & Ashby 1983; Cooper & Kohlstedt 1984; Karato *et al.* 1986; Kohlstedt & Chopra 1994), so the partially molten source rock can compact in response to melt flow (McKenzie 1984). Compaction provides space for the melt to accumulate in the source region (Jackson *et al.* 2003, 2005).

Geochemical models of continental crust evolution generally neglect segregation; they assume either the end-member of fractional melting, in which melt is instantaneously removed from the residual matrix as it forms and the bulk composition of the residual solid changes, or batch melting, in which there is no segregation of melt and matrix, melt remains in contact with the residual crystals and the bulk composition is constant. (e.g. Rollinson 2006). In the mantle, the generation of MORB has been described by polybaric partial melting models, in which individual batches of melt are generated over a range of depths during adiabatic upwelling of the mantle (e.g. Klein & Langmuir 1987; McKenzie & Bickle 1988). These batches of melt then segregate and ascend through the mantle to the base of the crust, where they mix to yield MORB compositions. In this scenario, the batches of melt apparently do not interact chemically with the mantle during ascent, which suggests that they must migrate through melt channels, pipes or fractures, rather than along grain boundaries (Spiegleman & Kenyon 1992). The chemical compositions of individual batches of melt are typically predicted from batch melting experiments, although it has recently been recognised that these experiments do not account for the depletion of the solid phase as melting proceeds, so experiments have been designed which attempt to capture the close to fractional nature of polybaric melting (e.g. Kinzler & Grove 1992; Kinzler 1997; Kushiro 2001).

In the continental crust, numerical models suggest that the steep thermal gradient through the source region will dominate the compositional evolution of melt and matrix; pressure variations are small because of the restricted vertical extent over which melting occurs (e.g. Hodge 1974; Bergantz 1989; Bergantz & Dawes 1994; Jackson *et al.* 2003). If melt segregates via fractures, which efficiently drain melt before it has interacted with the matrix, then segregated melt compositions may approach the limit of fractional melting. Batches of melt from different depths may mix, yielding something akin to a fractional 'polythermal' melting model. However, if melt flows along grain boundaries, then it will migrate through a temperature field which varies spatially and temporally, whilst interacting thermally and chemically with the surrounding matrix. The local bulk composition will change as melt migrates into, and out of, different regions. Melt and matrix are likely to reach local thermodynamic equilibrium during segregation, except for very high melt flow rate or low component diffusivity in the solid phase (Jackson *et al.* 2005). Consequently, there will be a continuous exchange of components between melt

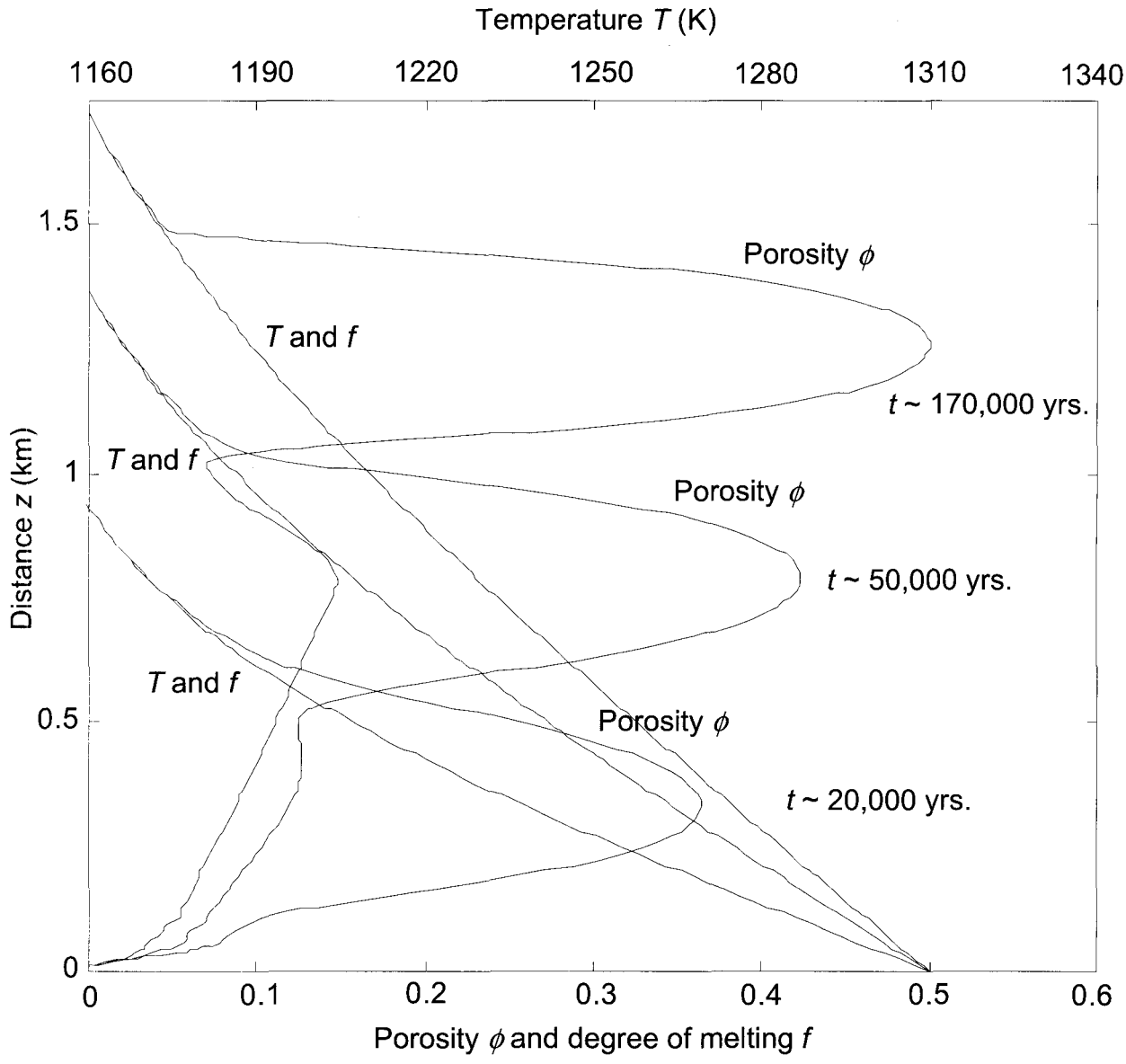

Figure 2 Melt volume fraction (porosity ϕ) and temperature (T) (also equilibrium degree of melting, f) versus vertical distance from the heat source (basaltic sill), after 20 000, 50 000 and 170 000 years following the onset of melting. The contact between source rock and underlying sill is at $z=0$. At time $t=0$ the sill is intruded, increasing the temperature of the overlying source rock and causing partial melting. The temperature at the contact is dictated by the thermal properties and initial temperature of the source rock and sill; in this example, it remains fixed at 1040°C (equivalent to $f=0{\cdot}5$) because cooling from the underlying sill does not reach the margin. Note the high porosity zone which develops in the source region over time. The composition of the melt in this zone can be estimated in terms of the equilibrium degree of melting (f). For example, after 170 000 years, the melt in the leading high porosity zone occupies c. 50 vol.% of the source rock, but its composition corresponds to only c. 8 vol.% melting of the host rock. However, using batch melting experiments to estimate composition introduces an error, because they do not account for the changing bulk composition as melt accumulates. Porosity (ϕ) and degree of melting (f) are read from the lower abscissa axis; temperature (T) is read from the upper abscissa axis.

and matrix as each migrates and equilibrates at new local conditions of temperature and bulk composition.

It is difficult to see how batch melting experiments can capture the evolution of melt and matrix chemistry during segregation in this dynamic melting environment. The implications of this are not clear. How might melt and residual matrix phase relations and composition be affected if segregation occurs along grain boundaries? Major, trace and REE compositions of both Archaean TTGs and modern adakite-like magmas have been used in conjunction with batch melting experiments and models to infer source rock compositions, depths of melting and tectonic setting. Could these be wrong? Do the physical processes by which melt segregates from, and interacts with, its partially molten host have a profound impact on the volume or composition of the segregated melt which leaves the source region?

The aim of this paper is to show how an experimental approach, when coupled with a numerical model, allows some of these issues to be addressed. The experiments are designed to reproduce the local changes in bulk composition that are predicted to occur in response to melt segregation along grain boundaries during partial melting of mafic lower crust, following the numerical model of Jackson *et al.* (2003, 2005). This model is investigated because it is the only one currently available which can quantitatively predict the local temperature and bulk melt composition during segregation. It is not claimed to capture the full complexity of the melt segregation processes but it is nonetheless a reasonable first step.

https://doi.org/10.1017/S0263593300001486 Published online by Cambridge University Press

Table 1 Nomenclature for the melt segregation model, along with likely ranges of values of the governing parameters for a basaltic protolith in the lower crust, and the values used in Figure 2

Symbol	Description	Minimum–maximum values	Values in Figure 2	Units
a	matrix grain radius	5×10^{-4}–5×10^{-3} (0·5–5 mm)	$2{\cdot}5 \times 10^{-3}$ (2·5 mm)	m
b	constant in permeability relation	1/2500–1/50	1/500	None
CMF	Critical Melt Fraction	0·4–0·65	0·5	None
c_{eff}	effective specific heat capacity $=c_p+L/(T_{liq}-T_{sol})$	2020–4220	3200	J kg^{-1}K^{-1}
c_p	specific heat capacity	1020–1220	1200	J kg^{-1}K^{-1}
f	equilibrium degree of melting	—	—	None
k	thermal conductivity	1·5–3	2	W K^{-1}m^{-1}
L	latent heat of fusion	400 000–600 000	600 000	J kg^{-1}
n	exponent in permeability relation	3	3	None
T_{liq}–T_{sol}	liquidus–solidus interval	200–400	300	K
T_{sill}	initial (intrusion) temperature of magma in sill		1460	K
δ	compaction lengthscale $=\left(\frac{(\xi_s+4\mu_s/3)ba^2\varphi^n}{\mu_m}\right)^{1/2}$	0·05–800	125	m
ϕ	porosity	—	—	None
φ	initial degree of melting at the contact $=\frac{T_{sill}-T_{sol}}{2(T_{liq}-T_{sol})}$	$\leq$0·5	0·5	None
κ_{eff}	dimensionless effective thermal diffusivity	10^{-5}–10^{+8}	3·56	None
μ_m	melt shear viscosity	10^3–10^6	10^4	Pa s
μ_s	matrix shear viscosity	10^{15}–10^{19}	10^{17}	Pa s
ρ	density	2900–3100	3000	kg m^{-3}
ρ_s ρ_m	matrix-melt density contrast	400–700	600	kg m^{-3}
ξ_s	matrix bulk viscosity	10^{15}–10^{19}	10^{17}	Pa s
τ	compaction timescale $=\frac{1}{(1-\varphi)(\rho_s-\rho_m)g}\left(\frac{\mu_m(\xi_s+4\mu_s/3)}{ba^2\varphi^n}\right)^{1/2}$	1×10^{10}–1×10^{14} (35yrs–3·5My)	$2{\cdot}67 \times 10^{11}$ (8450yrs)	

First, the segregation model of Jackson *et al.* (2003, 2005) is reviewed briefly. An experimental method is then described, designed to investigate the effect of melt segregation on phase relationships and melt and matrix compositions. Some preliminary results are presented, and their implications are discussed in terms of the application of batch melting experiments, and the origin and evolution of TTG magmas. It is suggested that an integrated physical and chemical approach may help to resolve the controversy surrounding the origin of TTGs.

1. Buoyancy driven melt segregation in the source region

Jackson *et al.* (2003, 2005) considered partial melting caused by the intrusion of hot, mantle derived basaltic magma into basaltic lower crust (Fig. 1). Basaltic and meta-basaltic rocks are regarded as protoliths for trondjhemite–tonalite–granodiorite (TTG) suites (e.g. Rapp *et al.* 1991; Rapp & Watson 1995; Martin 1999). Their model describes buoyancy-driven melt migration along grain boundaries, and associated compaction of the partially molten protolith. It omits external tectonic forces and fractures, and represents one end-member of a spectrum, at the other ends of which are models in which melt segregation is driven by deformation rather than buoyancy, and models in which melt segregation occurs via connected fracture networks rather than along grain-edges.

In their model, the source rock is initially solid. At time zero, the intrusion of magma causes partial melting of the overlying rock. This zone of partial melting is the source region; its top is defined by the position of the solidus isotherm and its base by the contact with the underlying magma. As heat is transferred into the source region its thickness increases: the position of the solidus isotherm migrates upwards away from the heat source. The melt is compositionally and thermally buoyant, so migrates upwards along grain boundaries towards the top of the source region. The partially molten source rock compacts in response.

As the melt migrates upwards along grain boundaries, it thermodynamically equilibrates with compacting matrix migrating downwards. This has two important consequences; the melt cannot migrate beyond the position of the solidus isotherm, which acts like a 'lid' on the top of the source region, and the composition of the melt continually evolves as it migrates upwards. Because it is equilibrating with cooler matrix, its composition evolves to approximately correspond to a smaller degree of equilibrium melting of the source rock.

When melt migrates upwards more quickly than the position of the solidus isotherm (the 'lid'), it accumulates near the top of the source region, where the matrix dilates to accommodate it. Jackson & Cheadle (1998) showed that the relative upward transport rates of heat and mass (melt) are described by a key dimensionless parameter, which they termed the 'effective thermal diffusivity' and which is given by

$$\kappa_{eff}=\frac{k\tau}{\rho c_{eff}\delta^2}$$

where k is the thermal conductivity, ρ is the density, c_{eff} is an effective specific heat capacity which accounts for the latent heat of fusion, and δ and τ are the characteristic compaction length- and time-scales of McKenzie (1984). Table 1 gives a description of these terms and likely values. The effective thermal diffusivity contains all of the key physical parameters which dictate the rates at which heat transport (via diffusion, which dominates advection as shown by Jackson & Cheadle 1998) and mass transport (via buoyancy driven melt flow along grain boundaries) occur. However, the predicted value of the effective thermal diffusivity for a basaltic source rock in the lower crust can vary by over twelve orders of magnitude,

https://doi.org/10.1017/S0263593300001486 Published online by Cambridge University Press

principally because of uncertainty in physical parameters such as the melt shear viscosity, the matrix bulk and shear viscosities and the matrix grain size, which appear in the expressions for the compaction length (δ) and time (τ) (see Table 1). Most values of the effective thermal diffusivity lie between 10^{-1} and 10^{6}. For values in the range 10^{-2} to 10^{4}, mass transport is rapid compared to heat transport, and melt accumulates at or near the top of the source region to form a high porosity zone (Fig. 2). When sufficient melt accumulates, the melt fraction (porosity ϕ) in this zone exceeds the CMF, the matrix disaggregates, and a mobile magma forms which may migrate away from the source region and be emplaced at shallower levels. Segregation is predicted to occur over time-scales ranging from 4000 yrs. to 10 M.y. with some values extending up to 50 M.y. Short segregation times indicate that batches of magma may be generated by only a few underplating events, so repeated underplating will yield numerous individual batches. Longer segregation times indicated that repeated underplating will be required to yield a single, large batch of magma, while very long segregation times suggest that the melt would not leave the source region for this combination of physical parameters.

For a given source rock and depth of melting, Jackson *et al.* (2003, 2005) used the results of published batch melting experiments (e.g. Beard & Lofgren 1991; Rapp *et al.* 1991, 1999; Rapp & Watson 1995) to predict melt and matrix compositions during segregation in terms of the local equilibrium degree of melting (f). This is not the same as the local melt fraction (ϕ), because the local melt fraction changes as melt migrates upwards and accumulates at the top of the source region. Rather, it is a measure of the fraction of the host rock which has melted, and depends only upon the local temperature, pressure, and bulk composition. The melt fraction (ϕ) and degree of melting (f) are the same if no melt migration occurs. Jackson *et al.* (2003, 2005) found that for a basaltic protolith melting at 1·0 to 3·2 GPa, the melts which accumulate to form a magma at high melt fraction (ϕ) at or near the top of the source region, represent only small degrees of equilibrium melting (f) of the source rock. Moreover, they correspond, at least approximately, to TTG compositions. This is a key finding of their work; not only does melt segregate within reasonable timescales, but the chemical evolution of the melt as it migrates upwards yields TTG compositions.

Their results suggest that buoyancy driven compaction with melt flow along grain boundaries can yield large volumes of segregated TTG melt over geologically realistic timescales. However, as Jackson *et al.* (2005) point out, their predicted melt compositions are not exactly correct, most significantly because the local bulk composition changes due to the relative movement of melt and matrix. They suggest that the approach may be reasonable for major elements due to their close to eutectic behaviour, but it is not clear whether this is the case. What is required is a method of replicating the change in bulk composition which occurs in the high porosity zone near the top of the source region, where large volumes of melt accumulate and thermodynamically equilibrate with matrix at relatively low temperatures. Such an experimental methodology is described in the following section.

3. Experimental study

3.1. Experimental representation of melt segregation

The numerical model predicts a combination of melt migration and chemical reaction through a steep thermal gradient. Hot melt migrating upwards thermodynamically equilibrates with cool matrix migrating downwards, so the compositions of both

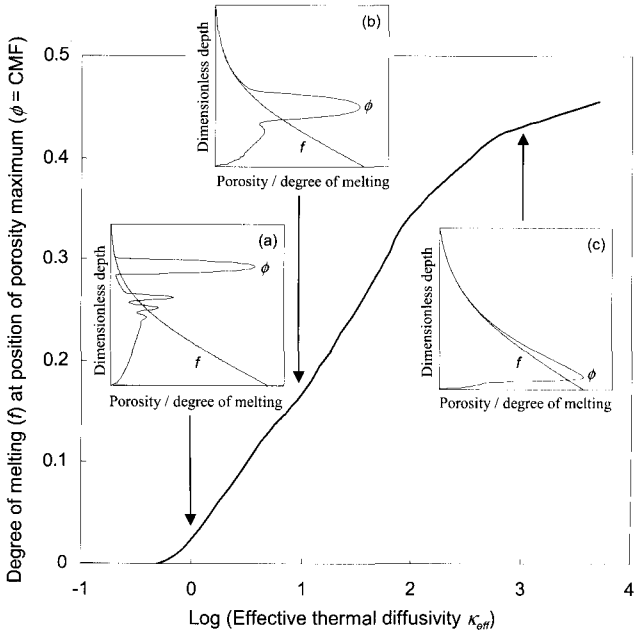

Figure 3 Equilibrium degree of melting (f) in the high porosity zone (at the depth where porosity ϕ=CMF), as a function of dimensionless effective thermal diffusivity (κ_{eff}). For a given source rock type, the composition of the segregated melt in the high porosity zone depends upon the local temperature, pressure and bulk composition, which is represented by the local equilibrium degree of melting (f). The location of the high porosity zone depends upon the physical parameters which govern heat and melt transport during segregation. These are captured by the value of κ_{eff} (equation 1; Jackson & Cheadle 1998; Jackson *et al.* 2003). For small values of κ_{eff}, melt transport is rapid relative to heat transport, so melt accumulates close to the top of the source region where the temperature is low, so the composition of the segregated melt corresponds to a small degree of equilibrium melting of the source rock (e.g. inset plot (a)). With increasing κ_{eff} the rate of melt transport decreases relative to the rate of heat transport, so melt accumulates closer to the base of the source region (inset plots (b) and (c)) and the composition of the segregated melt corresponds to an increasing degree of equilibrium melting of the source rock. The value of κ_{eff} is uncertain even for a given source rock composition (e.g. Table 1). Inset plots (a)–(c) show equilibrium degree of melting (f) and porosity (ϕ) as a function of dimensionless depth, captured at the time when maximum porosity ϕ=CMF (so magma formation is imminent), for (a) κ_{eff}=1; (b) κ_{eff}=10, and (c) κ_{eff}=1000. The top of each plot corresponds to the top of the source region, and the base to the contact between the source rock and the underlying magma heat source. The data shown in the main figure are obtained from numerous plots such as these.

continually evolve: higher temperature components freeze out of the melt, while lower temperature components melt out of the matrix. This yields melt compositions at the top of the source region (where temperatures are low) which correspond to small degrees of equilibrium partial melting ($f \leq$ 5–15 vol.%) of the source rock, but which have accumulated in large volumes in a zone of high porosity (ϕ>40 vol.%). For example, in Figure 2, the melt in the leading high porosity zone (at 170 000 yrs following the onset of melting) has accumulated to occupy a porosity ϕ=50 vol.% of the source rock, but has a composition equivalent to f=9 vol.% equilibrium partial melting.

This is reproduced experimentally in the following way. First, a normal equilibrium (batch) partial melting experiment is conducted on a natural basaltic bulk starting composition, at pressures appropriate for deep crustal melting (>1·0 GPa). This is termed a 'direct partial melting' (DPM) experiment. A temperature is chosen which will yield the same degree of equilibrium melting (f) as that predicted in the high porosity zone by the numerical model. For example, if the wish is to experimentally investigate melt composition in the high

https://doi.org/10.1017/S0263593300001486 Published online by Cambridge University Press

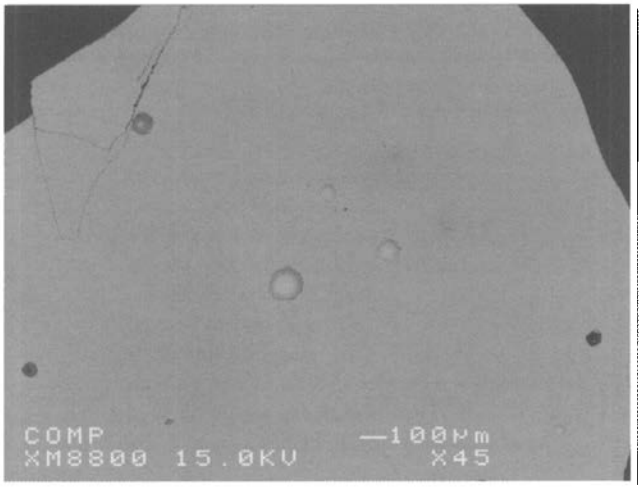

Figure 4 BSE image of synthetic glass SC5-8-1. Sample was made in a 1-atm furnace in the experimental petrology laboratory of D. R. Baker at McGill University. Glass was made from reagent grade chemical powders mixed together in the modal wt.% to produce the desired major element partial melt bulk composition, then melted at 1550°C, quenched, re-ground and then re-melted at 1550°C for 2 hours.

Table 2 Normalised weight percent compositions of starting materials. SC5 is a metamorphosed basaltic dike sample collected at Selwyn Creek, Fiordland, New Zealand. SC5-6 and SC5-8 are the melt compositions resulting from DPM experiments on the starting material at 5 and 15 vol.% partial melt, respectively. These compositions were used to make the synthetic glasses SC5-6-1 and SC5-8-1. The table lists the averages of the synthetic compositions determined by electron microprobe analyses. Mg.# of the glasses are also given

Oxides (wt.%)	SC5 bulk	SC5-6*	SC5-6-1	SC5-8**	SC5-8-1
SiO_2	46·44	76·06/75·29		67·49/67·13	
TiO_2	1·80	0·11/0·01		0·44/0·10	
Al_2O_3	18·89	15·28/15·84		18·18/18·89	
FeO	12·34	1·33/1·38		2·85/3·05	
MnO	0·20	0·04/0·01		0·07/0·05	
MgO	4·93	0·36/0·39		0·61/0·63	
CaO	9·09	2·10/2·19		3·26/3·56	
Na_2O	4·16	1·48/1·43		3·28/3·07	
K_2O	0·77	3·12/3·06		2·97/2·89	
P_2O_5	0·54	0·07/not add		0·27/not add	
SrO	neg	0·01/not add		0·12/not add	
Total	99·16	100·00/100·00		100·00/99·37	
Mg.#†		32		27	

*SC5-6: Partial melt at 850°C and 1·4 GPa representing 2–5 vol.% melt from bulk SC-5 normalised to 100.
**SC5-8: Partial melt at 975°C and 1·4 GPa representing 15 vol.% melt from bulk SC-5 normalised to 100.
†Mg.# = 100 × Mg/(Mg+Fe) molecular.

porosity zone shown in Figure 2 after 170 000 yrs, a temperature is chosen that yields a degree of melting of $f=9$ vol.%. The solid phase mineralogy and partial melt composition for this degree of melting are then determined. A synthetic glass that represents this partial melt composition is made.

The starting materials are now in place for the next partial melting experiment, which is termed a 'melt segregation equilibrium' (MSE) experiment. In this, the depleted solid phase obtained from the DPM experiment is mixed with the synthetic glass that represents the partial melt, in the same proportions as predicted by the numerical model. This is determined by the porosity in the high porosity zone where the low degree partial melt has accumulated. For example, to reproduce the numerical results shown in Figure 2 after 170 000 yrs, synthetic glass (melt) would be added to occupy $\phi=50$ vol.% of the charge (ignoring the minor change in volume when the glass melts during the experiment). This captures the change in bulk composition associated with the accumulation of melt in the high porosity zone. The mixed charge is then melted to the same temperature and pressure as in the DPM experiment. The new phase proportions, solid phase mineralogy and partial melt composition are determined for this bulk composition and degree of melting. The introduction of a large volume of small degree partial melt into a melting zone is not an assimilation or hybridisation process, so the experimental approach of the present authors is different from those in which contrasting rock types are mixed (e.g. Castro *et al.* 1999).

The numerical results shown in Figure 2 represent only one possible melting scenario. Different combinations of physical parameters such as melt viscosity, matrix bulk and shear viscosity, and matrix permeability, yield different values of the effective thermal diffusivity (calculated using Equation 1; see Table 1 for predicted range of values), which in turn yield different melt distributions through time (see, for example, figs 3 and 9 in Jackson *et al.* 2003, and fig. 4 in Jackson *et al.* 2005). For a given source rock composition, the composition of the melt which accumulates in the high porosity zone and eventually forms a mobile magma, depends upon the position at which accumulation occurs within the source region, because this dictates the local temperature and hence equilibrium degree of melting. Consequently, even if a given source rock composition is assumed, uncertainty in the governing physical parameters, and hence the value of the effective thermal diffusivity, results in different predicted melt compositions in the high porosity zone. Numerical experiments demonstrate that the equilibrium degree of melting in the high porosity zone increases with increasing effective thermal diffusivity (Fig. 3). For small values of effective thermal diffusivity, the high porosity zone forms very close to the top of the source region where temperatures are close to the solidus temperature of the source rock, so the equilibrium degree of melting is small (Fig. 3; see also fig. 9c in Jackson *et al.* 2003). As the effective thermal diffusivity increases, the position of the high porosity zone shifts towards the base of the source region where temperatures are higher, so the equilibrium degree of melting increases (Fig. 3; see also fig. 9a in Jackson *et al.* 2003).

In the present preliminary study, there is no attempt to exhaustively investigate the melt compositions which result from the full range of equilibrium degree of melting predicted by the numerical model for a given source rock composition (Fig. 3). Rather a choice is made to investigate systems in which the equilibrium degree of melting in the high porosity zone corresponds to $f=5\%$ and $f=15\%$. It is also assumed that the porosity is approximately $\phi=50$ vol.% in the high porosity zone, as this corresponds to the CMF used by Jackson *et al.* (2003, 2005), and is consistent with the SLT of Rosenberg & Handy (2005). Once the porosity reaches this value, the matrix will disaggregate, yielding a mobile magma which can migrate away from the source region. Changing these assumptions will change the composition of the melt which equilibrates in the high porosity zone (because the equilibrium degree of melting is different), and also the bulk composition of the high porosity zone (because the porosity in the zone, and hence the proportions of melt and matrix, is different).

Finally, in this present study, a significant simplification is made to the experimental methodology described above. The original (undepleted) bulk starting composition is mixed with the synthetic glass in the MSE experiments, rather than using the depleted solid phase obtained from the associated DPM

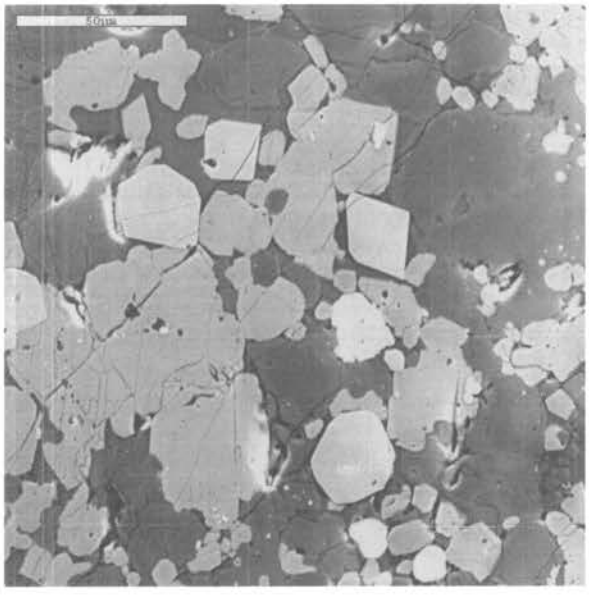

(a) SC5-8: 975°C, 1.4 GPa, 10 days (F-A)

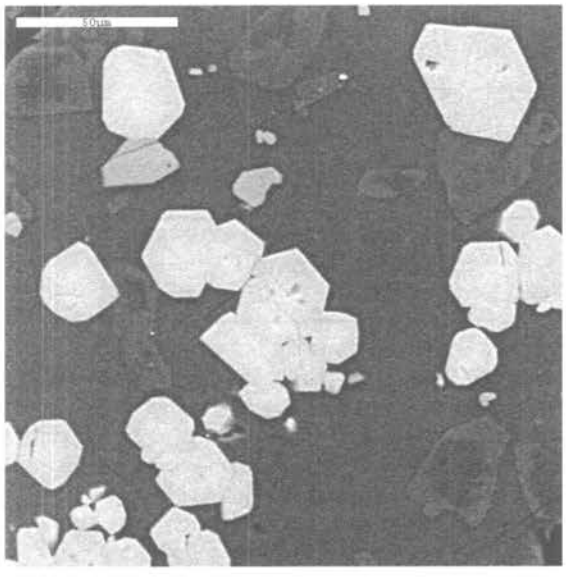

(b) (SC5(50)-3 (5%): 975°C, 1.4 GPa, 7 days, 2.5 H_2O

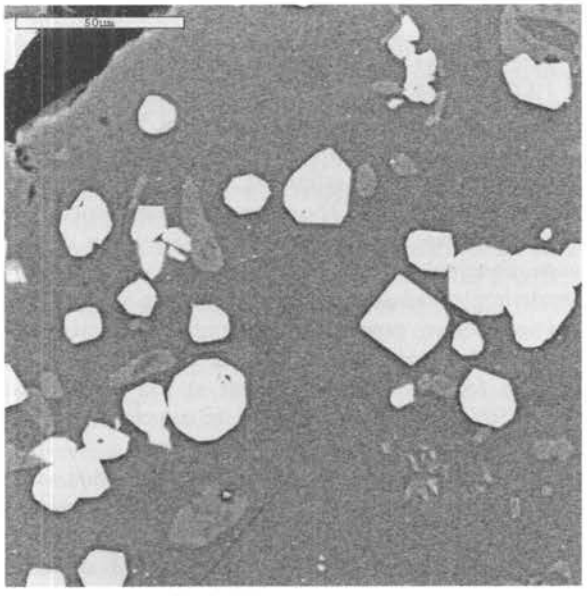

(c) SC5(50)-4 (15%): 975 °C, 1.4 GPa, 7 days, 2.5 H_2O

experiments. This means that the present experiments do not exactly match the numerical predictions, but they do allow the beginning of investigations into how segregating and accumulating a large volume fraction of low degree partial melt in the source region affects phase proportions, solid phase mineralogy and partial melt composition.

3.2. Starting materials: bulk compositions and synthetic glasses

A well-studied basaltic dike material (SC5, collected at Selwyn Creek, Fiordland, New Zealand) has been used for this initial study. It is an aphanitic dike, classified as basalt; the starting mode is presented in Table 2 (SC-5 Bulk). SC5 was the subject of a phase equilibria study at 1·4 GPa by Price (2004). Both major and trace elements were collected on experimental run products by electron probe and LA–ICPMS. This study comprises the DPM step of the methodology described above, and yields partial melt compositions representing $f=5$ vol.% melting (SC5-6), and $f=15$ vol.% melting (SC5-8). These are also shown in Table 2.

The next step is to prepare synthetic glasses for these two partial melt compositions. This was done at McGill University in Professor D. R. Baker's laboratory. Reagent grade chemical powders were used, mixed together in the appropriate percentages to produce the major element partial melt composition. The synthetic glasses were produced in a 1-atm furnace melted at 1550°C for 2 hours, then after quenching and re-grinding, re-melted under the same conditions to facilitate homogeneity. The glasses were checked by probe and shown to be homogeneous (Fig. 4). The average compositions of the synthetic glasses (from 5 analyses on each) are given in Table 2 (SC5-6-1 for the 5% melt and SC5-8-1 for the 15% melt).

The natural bulk composition and the synthetic glasses were then hand ground separately in an agate mill to 10 microns and mixed together in the desired proportions for the given experimental set. For this preliminary study, synthetic glasses and natural SC5 starting material were mixed in a 50:50 modal mix to represent a melt accumulation in which the porosity has increased to $\phi=50$ vol.% (e.g. Fig. 2). As the partial melts are also hydrous, 2–3 wt.% water was added to the charges (these partial melt compositions have between 4 and 6 wt.% water); the implications of the water contents are discussed below.

Geochemical analyses of the glasses and solid run product phases from the MSE experiments have been undertaken, with major element data being collected using the JOEL Microprobe housed at McGill University. Only major element data are shown in this present paper, but with glasses in equilibrium with garnet, HREE depletion in the glass would be expected.

3.3. Preliminary observations from melt segregation equilibrium experiments

Four sets of MSE experiments have been completed at 925°C, 950°C, 975°C and 1000°C and 1·4 GPa on the 50:50 mixtures of SC5 and the two synthetic glasses. The experiments were

Figure 5 BSE of experimental results. All scale bars are 50 μ. (a) Direct partial melting under fluid-absent (F-A) conditions. Hbd (moderate reflectivity, large grains) are present with garnet (higher reflecting roundish grains, plagioclase (dark grey) and melt, now glass, the darkest reflectivity and located in the upper right-hand corner. Melt volume is 15 vol.%. (b) SC(50)-3 run with 50:50 mix of SC5 and 5% partial melt composition (SC5-6-1). Melt volume is >50 vol.% and new product phases cpx and garnet (most reflective phases, with garnet slightly more reflective) co-exist with plagioclase (shows relief in the matrix) and glass (most of the matrix). (c) SC5(50)-4 run with 50:50 mix of SC5 and 15% partial melt composition (SC5-8-1). Cpx and garnet co-exist with plagioclase and glass. Melt volume is 50–55 vol.%.

https://doi.org/10.1017/S0263593300001486 Published online by Cambridge University Press

Table 3 Experimental glass compositions (unnormalised) in MSE experiments SC5(50)-1 through 8 performed at 925°C, 950°C, 975°C, 1000°C, 1·4 GPa are shown below in weight percent oxide. Mg.# of the glasses are also given

Oxides (wt.%)	925°C*[1] 1·4 GPa SC5(50)-1 5%	925°C 1·4 GPa SC5(50)-2 15%	950°C*[2] 1·4 GPa SC5(50)-7 5%	950°C 1·4 GPa SC5(50)-8 15%	975°C*[3] 1·4 GPa SC5(50)-3 5%	975°C 1·4 GPa SC5(50)-4 15%	1000°C*[4] 1·4 GPa SC5(50)-5 5%	1000°C 1·4 GPa SC5(50)-6 15%
SiO_2	67·19	68·05	65·73	64·12	65·92	64·41	66·59	62·36
TiO_2	0·13	0·10	0·27	0·37	0·64	0·55	0·38	0·21
Al_2O_3	14·76	14·70	14·63	16·03	14·78	15·93	14·81	16·61
FeO	1·35	1·31	1·71	2·41	2·45	2·18	2·41	2·12
MnO	0·03	0·03	0·02	0·04	0·01	0·01	0·03	0·07
MgO	0·55	0·49	0·87	0·79	0·74	0·62	0·89	1·34
CaO	2·53	2·35	2·8 5	3·21	3·65	2·73	3·44	3·66
Na_2O	2·19	2·44	2·68	3·14	2·77	3·66	2·57	3·35
K_2O	3·64	3·59	3·32	3·09	2·66	3·10	2·83	2·83
P_2O_5	0·18	0·15	0·25	0·31	0·23	0·20	0·31	0·45
Total	92·55	93·21	92·33	93·51	93·85	93·39	94·26	93·00
Mg.#	42	40	47	36	35	34	40	53

*[1]925°C, 1·4 GPa, SC5(50)-1,2: Partial melts in MSE experiments with 50:50 mix of 5% SC5(50)-6 and 15% SC5(50)-5 composition with SC5 starting material.
*[2]950°C, 1·4 GPa, SC(50)-7,8: Partial melts in segregation experiments with 50:50 mix of 5% SC5(50)-7 and 15% SC5(50)-8 composition with SC5 starting material.
*[3]975°C, 1·4 GPa, SC(50)-3,4: Partial melts in segregation experiments with 50:50 mix of 5% SC5(50)-4 and 15% SC5(50)-3 composition with SC5 starting material.

Table 4 Estimated modes by point-counting of solid phases and glass for the DPM experiments on SC5 at 925°C, 950°C and 975°C. Modes for the MSE experiments at 925°C, 950°C and 975°C with 15% partial melt composition added at 50% are given for comparison. Modes are in volume percent

Phase	SC5 starting mode	SC5-6 925°C DPM	SC5(50)-6 925°C 15% MSE	SC5-20 950°C DPM	SC5(50)-7 950°C 15% MSE	SC5-8 975°C DPM	SC5(50)-4 975°C 15% MSE
Plagioclase	45%	45%	38%	42%	26%	38%	22–25%
Hornblende	40%	40%	6%	38%	1%	30%	0%
Glass	0%	3–5%	27%	5%	48%	15%	50–55%
Garnet	0%	3–5%	12%	5–7%	6–10%	15%	13–20%
Clinopyroxene	<1%	0%	13%	0%	13–17%	5%	5–10%
Biotite	5%	0%	0%	0%	0%	0%	0%
Epidote	3–5%	0%	0%	0%	0%	0%	0%
Oxides	3–5%	5%	4%	5–8%	2%	5%	1–2%

run for 10, 7, 7 and 5 days respectively. These initial experiments are exploratory in that a range of temperatures was used for the MSE experiments, rather than the temperature that corresponded to the equivalent DPM experiment, so that preliminary data could be gathered. These initial observations are described, and then the focus is mainly on the results at 975°C for both the DPM and MSE experiments SC5-8 and SC5(50)-4 respectively. These are the best two experiments to compare in detail, because the melting temperature in the MSE experiment is consistent with the degree of melting in the DPM experiment. This allows direct comparison of the resulting glass compositions and modes to investigate the impact of melt segregation on melt chemistry and volume.

Two charges simultaneously can be loaded into the piston-cylinder, and this set-up is used to run both compositions of synthetic glass mixed with the natural metabasalt.

3.4. Experimental melt compositions and volumes

Table 3 shows the partial melt compositions and Mg-numbers (100 × Mg/(Mg+Fe) molecular) produced in the MSE experiments. These should be compared with the DPM partial melt compositions and Mg-numbers in Table 2. Table 4 compares modes from both DPM and MSE experiments run at 925°C, 950°C and 975°C, and the starting mode for SC5.

Figure 5 shows images from MSE experiments at 975°C and 1·4 GPa (SC5(50)-3 and SC5(50)-4), and compares them with that found in DPM experiments of SC5 under the same P–T conditions (Price 2004). The modes for the different MSE experiments have been estimated by point-counting back-scatter images (Table 4). The decrease in hornblende stabilisation and increase in clinopyroxene stabilisation is the largest change observed in the MSE experiments, along with a decrease in plagioclase mode and an increase in garnet mode. Glass volumes are expected to be significantly increased over that in DPM experiments at the same temperature. A simple prediction for the MSE experiment at 975°C is: 50 vol.% added +(50%*15%) from melting of the source material would yield ~57·5 vol.%. We observe 50–55 vol.%.

Generally a change is seen in the melt composition and melt and solid phase modes between DPM and MSE experiments. In Figure 6, the new MSE data is plotted in an Ab–An–Or diagram, along with the experimental DPM data (Price 2004) and Separation Point Batholith data from Tulloch & Kimbrough (2003), which is a natural and well documented

https://doi.org/10.1017/S0263593300001486 Published online by Cambridge University Press

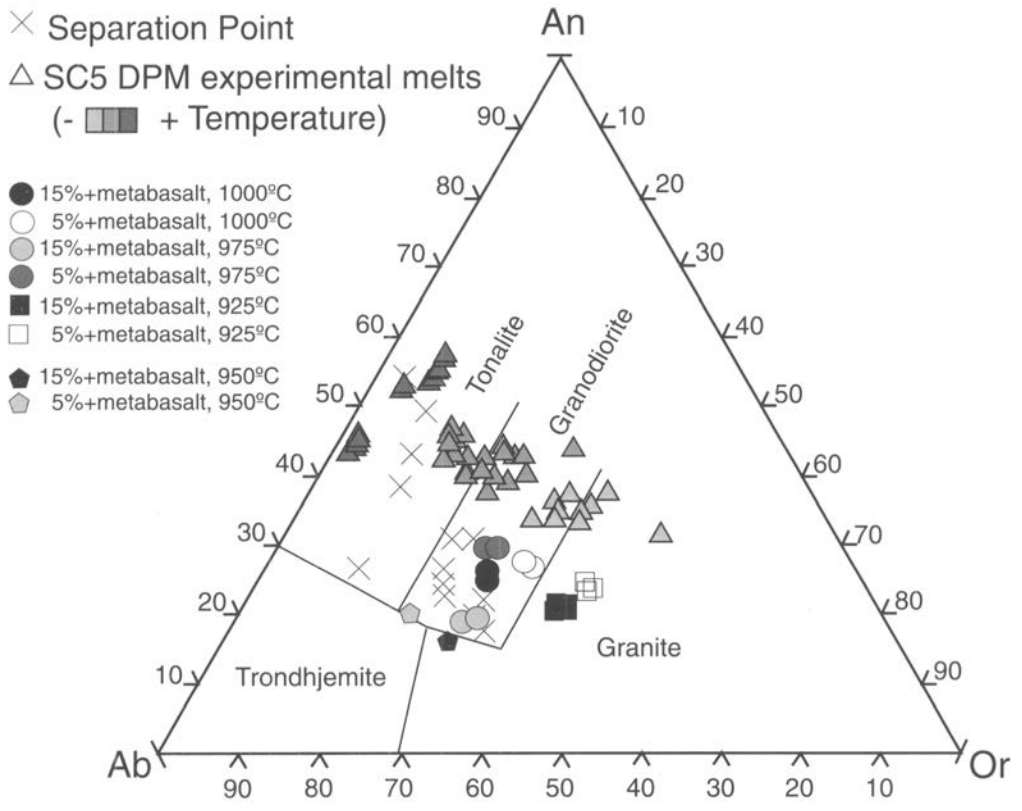

Figure 6 Glass data from the four sets of MSE experiments run at 925°C, 950°C, 975°C and 1000°C, 1·4 GPa are plotted as shaded circles on this Ab–An–Or plot. The shaded triangles are the 925–1000°C melt compositions from direct partial melting of SC5. The crosses are natural data from Separation Point Batholitic Complex (Tulloch & Kimbrough 2003).

example of a large TTG batholith with a depleted HREE and high Sr/Y ratio chemical signature. The MSE experiments are enriched in Ab and Or components in comparison with the DPM results. In comparing and contrasting 975°C results, the DPM melt compositions bridge the granodiorite and tonalite fields with a ca. 45% An component. However, the MSE experiments are lower in An component. The MSE SC5(50)-3 and 7 are most enriched in Ab–Or components with a ca. 20% An component. These experimental MSE melt compositions are dominantly granodioritic. The lowest temperature experiments plot in the granite field. The intermediate temperatures skirt the trondhjemite field.

Figure 7a plots Mg.# vs SiO_2 for MSE and DPM melt compositions along with the natural TTG range from Condie 2005. Figure 7b plots MgO vs. SiO_2 for MSE and DPM melt compositions, along with natural adakite compositions and the natural TTG field from Martin (1999). The Mg-numbers for the MSE experiments have increased over those in the direct melting experiments. For the 975°C experiment with 15% melt composition, the Mg-number increases from 27 for DPM to 34 in the MSE. The others increase to 40–42, with the 1000°C run with 15% melt composition increasing to 53 (Table 3).

4. Discussion

In this preliminary study, it is found that using a physics-based model may help in providing additional constraints to experimental studies on the origin of TTGs. Because a component of melt segregation is included, its impact on bulk composition can be investigated, and, therefore, phase equilibria during continued partial melting in a mafic source region. The preliminary results described above show how the geochemical system has been changed by segregating and accumulating a low-degree, partial melt in a metabasalt source material.

4.1. Melt volume

The preliminary data remain somewhat inconclusive in terms of melt volume generated in these experiments. Data from the 975°C MSE experiment show that the mode of melt increases to 50–55 vol.% compared with 15 vol.% generated from the DPM experiments. An increase in melt mode is expected, simply because 50% has been added to the charge to represent segregated melt accumulating in the source region. However, the melt mode recorded in the MSE experiments is consistently less than the 57·5% mode predicted by simple batch melting. A reduction in melt volume when compared to simple batch melting experiments is consistent with the results of fractional mantle melting experiments, that show reduced melt volumes compared to batch melting (Kushiro 2001). However, the reasons are different. Early models of polybaric melting in the mantle assumed a constant source rock composition during decompression melting and segregation (Klein & Langmuir 1987; McKenzie & Bickle 1988). In reality, the bulk composition changes during mantle upwelling, becoming less fertile as early melting phases are extracted (Kinzler & Grove 1992; Kushiro 2001). In these experiments, fertility is modified by changing bulk composition, then re-establishing new equilibria which changes the solid phase assemblage. These different variables will all have an effect on melt volume and melt water content.

Currently, approximately 2·5 wt.% water is added to the MSE experiments. This may be too low, and it is necessary to consider higher contents to replicate low degree hydrous partial melts. The 2·5 wt.% added into these experiments is

https://doi.org/10.1017/S0263593300001486 Published online by Cambridge University Press

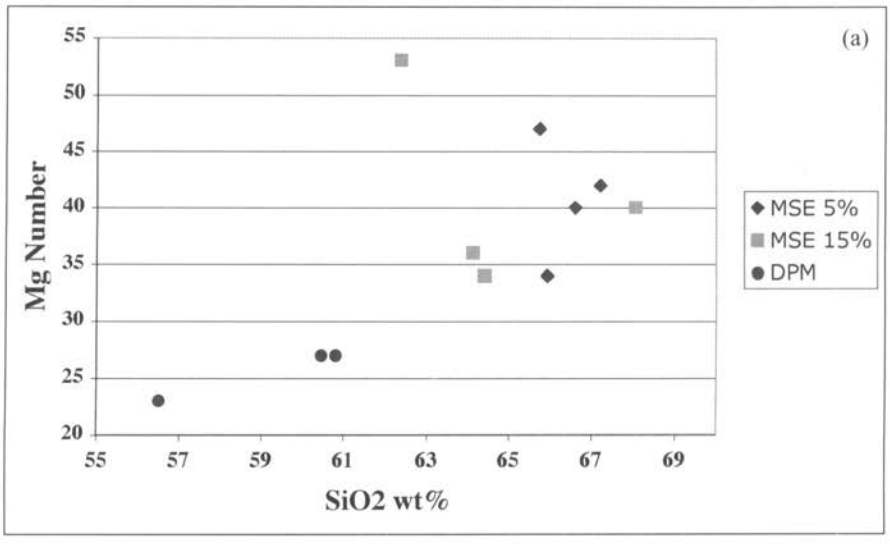

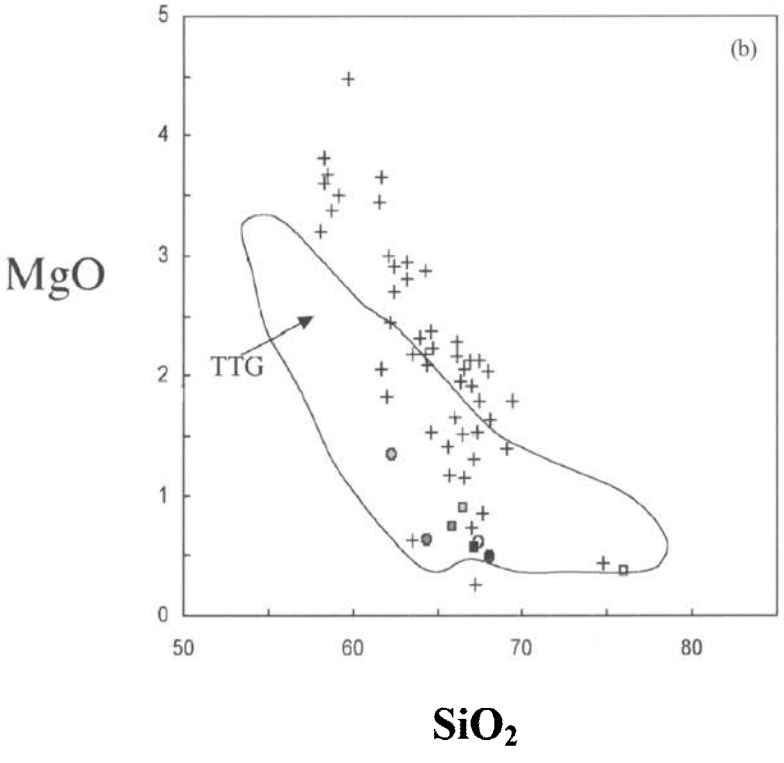

Figure 7 (a) Mg number versus SiO_2 for the MSE and DPM experiments. Data are listed in Table 3. The increase in Mg number in the MSE experiments (squares and diamonds) compared with the DPM experiments (circles) is seen as mainly a reflection of a change in the solid phase assemblage, with the decreasing stability of hornblende with respect to garnet and clinopyroxene. The natural TTG field is given for the range of SiO_2 and Mg numbers shown in the plot. Data from Condie 2005. (b) MgO vs SiO_2 for the MSE and DPM experiments. Open square/circle are the DPM experiments (square = 5% and circle = 15% partial melt mix). Shaded square/circle are the MSE experiments (darker shading is for lower temperature runs and paler shading is for higher temperature runs). The field of TTG is also added for comparison. Adakites, as noted by many workers, have higher MgO contents and are shown as crosses. Data from Martin (1999).

correct for those at 975°C, but is too low for lower degree partial melts which have higher water contents (Clemens & Vielzeuf 1987).

4.2. Melt composition

Overall, the resulting melt compositions in the MSE experiments are lower in the An component when plotted in an Ab–An–Or ternary, and have higher Mg-numbers when compared with the DPM results. Modally, the charges have changed too, with a reduction in hornblende and plagioclase and an increase in garnet and clinopyroxene as a function of increasing temperature. These changes are reflected in the melt compositions. The decrease in An shown in Figure 6, is likely a combination of a decrease in plagioclase stability and the addition of the low melt fraction compositions to the charges which have elevated alkalis. However, in this preliminary study sodic trondhjemite compositions have not been produced. The increase in garnet and clinopyroxene and the decrease in the stability of hornblende is seen in the melt composition as an increase in the Mg number. A more subtle effect is also related

https://doi.org/10.1017/S0263593300001486 Published online by Cambridge University Press

to the destabilisation of hornblende. There is an increase in FeO relative to MgO at 950°C and 975°C, so within a small range of temperatures, the Mg number decreases, although it is still higher than in the DPM experiments. It then continues to increase with increasing temperature (Table 3; Fig. 7a, b).

Figures 7a and b also show the natural range of TTG magmas in terms of MgO, Mg-number and SiO_2. TTGs, while similar to adakites in terms of La/Yb and Sr/Y ratios, exhibit important geochemical differences, particularly in terms of Mg, Cr and Ni, which are lower in some TTGs. In a review of literature and unpublished data on TTGs, Condie (2005) points out that high-Al TTGs may more likely be produced at depths where garnet is stable, in the presence of low-Mg hornblende, and low amounts of plagioclase. These data have also been used to participate in the debate on whether or not there is a systematic increase in Mg number, Cr, and Ni between 4 and 2·5 Ga. In addition, if this change is real, can it be tied to cooling thermal conditions of the Earth's mantle? The argument that there is an increase in Mg-number through time, has led Martin & Moyen (2002) to argue that TTGs interact more with the mantle wedge with time and as result suggest that all these magmas are slab-derived. However, compiled data by Condie (2005) suggests that there may not be such a systematic shift in Mg number, with the data showing a range in values during Earth's history with no obvious trends (e.g. Condie 2005, fig. 8).

If dynamic melt segregation and equilibrium processes such as those described here are active in lower mafic crust during arc growth, they may modify source bulk composition so that normally robust geochemical indicators, such as Mg number, are themselves affected. This raises the possibility that the high Mg numbers in adakites might be a segregation effect rather than a direct indication of mantle contamination. The results to date are preliminary, and only one basaltic source rock composition and two melt segregation scenarios have been investigated. Nevertheless, this is an area that deserves further investigation, as it has significant implications for the interpretation of geochemical data to infer source region settings and processes.

5. Summary

A coupled physical and chemical model has been presented that suggests that melt may segregate rapidly from a mafic host when it flows along grain boundaries due to buoyancy and the matrix compacts in response. A key factor in the segregation mechanism is the combination of melt migration and chemical reaction through a steep geothermal gradient, which causes the melt composition to evolve as it migrates, yielding TTG melt compositions which accumulate at the top of the source region and are free to ascend through the crust. A 'proof of concept' study has been embarked upon to investigate and quantify the effect of melt segregation on melt compositions. The preliminary results presented here suggest that dynamic melt segregation and equilibrium processes which may be active in mafic lower crust can modify source rock bulk composition, so that normally robust geochemical indicators are modified by the segregation process. This raises the possibility that the high Mg numbers in adakites might be a segregation effect rather than a direct indication of mantle contamination.

6. Acknowledgements

TR would like to thank Amanda Getsinger for experimental help and Don Baker for support and discussion and allowing us access to his piston-cylinder laboratory at McGill University.

7. References

Atherton, M. P. & Petford, N. 1993. Generation of a sodium-rich magma from newly underplated basaltic crust. *Nature* **362**, 144–6.

Beard, J. S. & Lofgren, G. E. 1991. Dehydration melting and water-saturated melting of basaltic and andesitic greenstones and amphibolites at 1, 3, and 6·9 kb. *Journal of Petrology* **32**, 365–401.

Bergantz, G. W. 1989. Underplating and partial melting: Implications for melt generation and extraction. *Science* **245**, 1093–5.

Bergantz, G. W. & Dawes, R. 1994. Aspects of magma generation and ascent in continental lithosphere. *In* Ryan, M. P. (ed.) *Magmatic Systems*, 291–397. London: Academic Press.

Brown, M. 1994. The generation, segregation, ascent and emplacement of granitic magma: The migmatite-to-crustally derived granite connection in thickened orogens. *Earth Science Reviews* **36**, 83–130.

Brown, M., Averkin, Y. A. & McLellan, E. L. 1995. Melt segregation in migmatites, *Journal of Geophysical Research* **100**, 15,655–79.

Brown, M. & Rushmer, T. 1997. Consequences of deformation-assisted melt segregation: New views from the field and the laboratory. *In* Holness, M. (ed.) *Deformation-enhanced melt segregation and metamorphic fluid transport*, 111–39. *Mineralogical Society Series.* London: Chapman & Hall.

Castro, A., Patiño Douce, A. E., Corretgé, L. G., de la Rosa, J., El-Biad, M., El-Hm, H. 1999. Origin of peraluminous granites and granodiorites, Iberian massif, Spain: an experimental test of granite petrogenesis. *Contributions to Mineralogy and Petrology* **135** (2–3), 255–76.

Clemens, J. D. & Vielzeuf, D. 1987. Constraints on melting and magma production in the crust. *Contributions to Mineralogy and Petrology* **107**, 41–59.

Condie, K. C. 2005. TTGs and adakites: are they both slab melts? *Lithos* **80**, 33–44.

Cooper, R. F. & Kohlstedt, D. L. 1984. Solution-precipitation enhanced diffusional creep of partially molten olivine-basalt aggregates during hot pressing. *Tectonophysics* **107**, 207–33.

Davidson, J. P. & Arculus, R. J. 2006. The significance of Phanerozoic arc magmatism in generating continental crust. *In* Brown, M. & Rushmer, T. (eds) *Evolution and Differentiation of the Continental Crust*, 135–72. Cambridge: Cambridge University Press.

Drummond, M. S. & Defant, M. J. 1990. A model for trondhjemite-tonalite-dacite gensis and crustal growth during slab melting; Archean to modern comparisons. *Journal of Geophysical Research* **95**, 21,503–21.

Gutscher, M. A., Maury, R., Eissen, J. P. & Bourdon, E. 2000. Can slab melting be caused by flat subduction? *Geology* **28**, 535–8.

Hodge, D. S. 1974. Thermal model for origin of granitic batholiths. *Nature* **251**, 297–9.

Jackson, M. D., Cheadle, M. J. & Atherton, M. P. 2003. Quantitative modeling of melt generation and segregation in the continental crust. *Journal of Geophysical Research* **108**, 2332–53. doi:10.1029/2001JB001050.

Jackson, M. D., Gallagher, K. Petford, N. & Cheadle, M. J. 2005. Towards a coupled physical and chemical model for tonalite–trondhjemite–granodiorite magma formation. *Lithos* **79**, 43–60.

Jackson, M. D. & Cheadle, M. J. 1998. A continuum model for the transport of heat, mass and momentum in a deformable mush, undergoing solid–liquid phase change. *International Journal of Heat and Mass Transfer* **41**, 1035–48.

Karato, S., Paterson, M. S. & FitzGerald, J. D. 1986. Rheology of synthetic olivine aggregates: Influence of grain size and water. *Journal of Geophysical Research* **91**, 8151–76.

Keleman, P. B., Rilling, J. L., Parmentier, E. M., Mehl, L. & Hacker, B. R. 2003. Thermal structure due to solid-state flow in the mantle wedge beneath arcs. *In* Eiler, J. (ed.) *Inside the Subduction Factory. American Geophysical Union Monograph* **138**, 293–311.

Kincaid, C. & Sacks, I. S. 1997. Thermal and dynamical evolution of the upper mantle in subduction zones. *Journal of Geophysical Research* **102**, 12295–315.

Kinzler, R. J. 1997. Melting of mantle peridotite at pressures approaching the spinel to garnet transition: Application to mid-ocean ridge basalt petrogenesis. *Journal of Geophysical Research* **102** (B1), 853–74.

Kinzler, R. J. & Grove, T. L. 1992. Primary magmas of mid-oceanic basalts 2: Applications. *Journal of Geophysical Research* **97**, 6907–26.

Klein, E. M. & Langmuir, C. H. 1987. Global correlations of ocean ridge basalt chemistry with axial depth and crustal thickness. *Journal of Geophysical Research* **92** (B8), 8089–115.

Kohlstedt, D. L. & Chopra, P. N. 1994. Influence of Basaltic Melt on the Creep of Polycrystalline Olivine under Hydrous Conditions. *In* Ryan, M. P. (ed.) *Magmatic Systems*, Chap. 3. London: Academic Press.

Kushiro, I. 2001. Partial melting experiments on peridotite and origin of mid-oceanic ridge basalt. *Annual Reviews of Earth and Planetary Sciences* **29**, 71–107.

Lupulescu, A. & Watson, E. B. 1999. Low-melt fraction connectivity of granitic and tonalitic melts in a mafic crustal rock at 800 °C and 1 GPa. *Contributions to Mineralogy and Petrology* **134**, 202–16.

Martin, H. 1999. Adakitic magmas: Modern analogues of Archean granitoids. *Lithos* **46**, 411–29.

Martin, H., Smithies, R. H., Rapp, R., Moyen, J.-F. & Champion, D. 2005. An overview of adakite, tonalite-trondhjemite-granodiorite (TTG) and sanukitoid: relationships and some implications for crustal evolution. *Lithos* **79**, 1–24.

Martin, H. & Moyen, J.-F. 2002. Secular changes in tonalite–trondhjemite–granodiorite composition as markers of the progressive cooling of Earth. *Geology* **30**, 319–22.

McKenzie, D. 1984. The generation and compaction of partially molten rock. *Journal of Petrolology* **25**, 713–65.

Mckenzie, D. & Bickle, M. J. 1988. Volume and composition of melt by extension of the lithosphere. *Journal of Petrology* **29**, 625–79.

McLennan, S. M., Taylor, S. R. & Hemming, S. R. 2006. Composition, differentiation and evolution of the continental crust: constraints from sedimentary rocks and heat flow. *In* Brown, M. & Rushmer, T. (eds) *Evolution and Differentiation of the Continental Crust*, 92–134. Cambridge: Cambridge University Press.

Peacock, S. M., Rushmer, T. & Thompson, A. B. 1994. Partial melting of subducting oceanic crust. *Earth and Planetary Science Letters* **121**, 227–43.

Petford, N. 1995. Segregation of tonalitic–trondhjemitic melts in the continental crust: The mantle connection. *Journal of Geophysical Research* **100**, 15,735–43.

Petford, N. 2003. Rheology of granitic magmas during ascent and emplacement. *Annual Review of Earth and Planetary Sciences* **31**, 399–427.

Petford, N. & Atherton, M. 1996. Na-rich partial melts from newly underplated basaltic crust: the Cordillera Blanca batholith, Peru. *Journal of Petrology* **37** (6), 1491–521.

Petford, N. & Koenders, M. A. 1998. Self-organisation and fracture connectivity in rapidly heated continental crust. *Journal of Structural Geology* **20**, 1425–34.

Pharr, G. M. & Ashby, M. F. 1983. On creep enhanced by a liquid phase *Acta Metallurgica* **31**, 129–38.

Pitcher, W. S. 1990. The nature, ascent and emplacement of granitic magmas. *Journal of the Geological Society, London* **136**, 627–62.

Price, R. P. W. 2004. *Testing the partial melting of a basaltic underplate: origin of Cretaceous granitoids in Fiordland, New Zealand.* MSc. Thesis, University of Vermont, Burlington, USA.

Rapp, R. P., Watson, E. B. & Miller, C. F. 1991. Partial melting of amphibolite/eclogite and the origin of Archean trondhjemites and tonalites. *Precambrian Research* **51**, 1–25.

Rapp, R. P., Shimizu, N., Norman, M. D. & Applegate, G. S. 1999. Reaction between slab-derived melts and peridotite in the mantle wedge: experimental constraints at 3·8 GPa. *Chemical Geology* **160**, 335–56.

Rapp, R. P. & Watson, E. B. 1995. Dehydration melting of metabasalt at 8–32 kbar: implications for continental growth and crust–mantle recycling. *Journal of Petrology* **36**, 891–931.

Richter, F. M. & McKenzie, D. P. 1984. Dynamical models for melt segregation from a deformable matrix. *Journal of Geology* **92**, 729–40.

Rollinson, H. 2006. Crustal generation in the Archean. *In* Brown, M. & Rushmer, T. (eds) *Evolution and Differentiation of the Continental Crust*, 173–230. Cambridge: Cambridge University Press.

Rosenberg, C. & Handy, M. 2005. Experimental deformation of partially melted granite revisited: implications for the continental crust. *Journal of Metamorphic Geology* **23**, 19–28.

Rushmer, T. 1991. Partial melting of two amphibolites: Contrasting experimental results under fluid-absent conditions. *Contributions to Mineralogy and Petrology* **107**, 41–59.

Rushmer, T. 2001. Volume change during partial melting reactions: Implications for melt extraction, melt geochemistry and crustal rheology. *Tectonophysics* **34** (2/3–4), 389–405.

Sawyer, E. W. 1994. Melt segregation in the continental crust. *Geology* **22**, 1019–22.

Sawyer, E. W. 1996. Melt segregation and magma flow in migmatites: implications for the generation of granitic magmas. *Transactions of the Royal Society of Edinburgh: Earth Sciences* **87**, 85–94.

Spiegleman, M. & Kenyon, P. 1992. The requirements for chemical disequilibrium during magma migration. *Earth and Planetary Science Letters* **109** (3–4), 611–20.

Tulloch, A. J. & Kimbrough, D. L. 2003. Paired plutonic belts in convergent margin and the development of high Sr/Y magmatism: The Peninsular Ranges Batholith of California and the Median Batholith of New Zealand. *Geological Society of America, Special Paper* **374.**

van der Molen, I. & Paterson, M. S. 1979. Experimental deformation of partially melted granite. *Contributions to Mineralogy Petrology* **70**, 299–318.

Vicenzi, E. P., Rapp, R. P. & Watson, E. B. 1998. Crystal/Melt Wetting Characteristics in Partially Molten Amphibolite. *EOS* **69**, 482.

von Bargen, N. & Waff, H. S. 1986. Permeabilities, interfacial areas and curvatures of partially molten systems: results of numerical computations of equilibrium microstructures. *Journal of Geophysical Research* **91**, 9261–76.

Wark, D. A. & Watson, E. B. 1998. Grain-scale permeabilities of texturally equilibrated, monomineralic rocks, *Earth and Planetary Science Letters* **164**, 591–605.

Wickham, S. M. 1987. The segregation and emplacement of granitic magmas. *Journal of the Geological Society, London* **144**, 281–29.

Wolf, M. B. & Wyllie, P. J. 1991. Dehydration melting of solid amphibolite at 10 kbar: Textural development, liquid interconnectivity and applications to the segregation of magmas. *Mineralogy and Petrology* **44**, 151–79.

Wolf, M. B. & Wyllie, P. J. 1994. Dehydration melting of amphibolite at 10 kbar: The effects of temperature and time. *Contributions to Mineralogy and Petrology* **115**, 369–83.

TRACY RUSHMER, Department of Geology, University of Vermont, Burlington, VT 05401, USA.
e-mail: Tracy.Rushmer@uvm.edu

MATT JACKSON, Department of Earth Science and Engineering, Royal School of Mines Building, Imperial College, London SW7 2BP UK.
e-mail: m.d.jackson@imperial.ac.uk

MS received 25 October 2006. Accepted for publication 1 August 2007.